Insulin Receptor Signaling in POMC, but Not AgRP, Neurons Controls Adipose Tissue Insulin Action

Andrew C. Shin, Nika Filatova, Claudia Lindtner, Tiffany Chi, Seta Degann, Douglas Oberlin, and Christoph Buettner

Diabetes 2017;66:1560–1571 | https://doi.org/10.2337/db16-1238

Insulin is a key regulator of adipose tissue lipolysis, and impaired adipose tissue insulin action results in unrestrained lipolysis and lipotoxicity, which are hallmarks of the metabolic syndrome and diabetes. Insulin regulates adipose tissue metabolism through direct effects on adipocytes and through signaling in the central nervous system by dampening sympathetic outflow to the adipose tissue. Here we examined the role of insulin signaling in agouti-related protein (AgRP) and proopiomelanocortin (POMC) neurons in regulating hepatic and adipose tissue insulin action. Mice lacking the insulin receptor in AgRP neurons (AgRP IR KO) exhibited impaired hepatic insulin action because the ability of insulin to suppress hepatic glucose production (hGP) was reduced, but the ability of insulin to suppress lipolysis was unaltered. To the contrary, in POMC IR KO mice, insulin lowered hGP but failed to suppress adipose tissue lipolysis. High-fat diet equally worsened glucose tolerance in AgRP and POMC IR KO mice and their respective controls but increased hepatic triglyceride levels only in POMC IR KO mice, consistent with impaired lipolytic regulation resulting in fatty liver. These data suggest that although insulin signaling in AgRP neurons is important in regulating glucose metabolism, insulin signaling in POMC neurons controls adipose tissue lipolysis and prevents high-fat diet–induced hepatic steatosis.

METABOLISM

The mediobasal hypothalamus (MBH) is a key brain region that assesses energy availability by sensing hormones and nutrients to coordinate energy homeostasis. Within the MBH, agouti-related protein (AgRP) and proopiomelanocortin (POMC) neurons play critical roles in ingestive behavior. Activation of AgRP neurons rapidly and markedly increases food intake (1–3), whereas ablation of AgRP neurons in adult mice results in profound starvation and weight loss (4–6). Activation of POMC neurons reduces appetite (7,8), whereas inhibition of POMC neurons modestly increases feeding (8).

The insulin receptor (IR) is expressed in both AgRP and POMC neurons. Although insulin has been shown to hyperpolarize and inhibit AgRP and POMC neurons (9–11), there are reports that insulin can also activate AgRP and POMC neurons (11,12), possibly as a result of heterogeneity among these neurons. Deletion of the IR from AgRP neurons (AgRP IR KO) results in mild hepatic insulin resistance (9), defined as the reduced ability of insulin to suppress hepatic glucose production (hGP). However, despite hepatic insulin resistance, the glucose infusion rate (GIR) required to maintain euglycemia during the hyperinsulinemic clamps was not altered in AgRP IR KO mice, and importantly, they were also able to maintain normal glucose tolerance (9), indicating that the impairment of hepatic insulin action was moderate. In contrast, deletion of the IR in POMC neurons (POMC IR KO mice) did not alter hGP or impair glucose tolerance when mice were fed a standard chow diet (9,13).

Brain insulin signaling controls white adipose tissue (WAT) metabolism by suppressing lipolysis and stimulating de novo lipogenesis, enabling WAT to store lipids (14,15). The ability of WAT to rapidly switch from a lipolytic state during fasting (which provides free fatty acids and glycerol to be used as energy substrates in organs such as muscle and liver) to a lipid storage mode after meal ingestion (which is important to prevent lipotoxicity) is critical for metabolic health and is reduced in

Diabetes, Obesity, and Metabolism Institute, Icahn School of Medicine at Mount Sinai, New York, NY

Corresponding author: Christoph Buettner, christoph.buettner@mssm.edu.

Received 11 October 2016 and accepted 22 March 2017.

A.C.S. is currently affiliated with Department of Nutritional Sciences, College of Human Sciences, Texas Tech University, Lubbock, TX.

metabolic syndrome and type 2 diabetes (16). High-fat diet (HFD) feeding rapidly impairs brain insulin action, resulting in impaired suppression of hGP and adipose tissue lipolysis and may lead to hepatic steatosis (17–20). Given the importance of WAT functionality for metabolic health, a better understanding of the neuronal pathways that mediate brain insulin action to control WAT lipolysis is needed.

Activation of melanocortinergic signaling induces WAT lipolysis through increased sympathetic outflow (21), indicating that POMC neurons participate in the sympathetic regulation of adipose tissue. The role of AgRP neurons in regulating adipose tissue metabolism is less well defined. The aim of our study was to examine the role of insulin signaling in AgRP and POMC neurons in regulating hepatic insulin action and adipose tissue lipolysis.

RESEARCH DESIGN AND METHODS

Animals

All mice used in this study were 3–4 months old. AgRP IR KO or POMC IR KO mice were generated by crossing mice floxed for the IR (14) (provided by Drs. Ronald Kahn and Jens Bruning) with mice expressing Cre recombinase in AgRP or POMC promoter (AgRP internal ribosome entry site Cre was provided by Dr. Joel Elmquist; Tg(Pomc1-cre)16Lowl/J, stock number 005965; The Jackson Laboratory, Bar Harbor, ME). Mice homozygous for IR flox and negative for Cre were used as controls. The mice were genotyped by PCR using genomic DNA isolated from tail tips as described previously (9). *AgRPCre* primers: *AgRPCre 5′*: 5′-CCCTAAGGATGAGGAGAGAC-3′; *Cre-intern-rev-3′*: 5′-ATGTTTAGCTGGCCCAAATGT-3′; *AgRP-Intron*: 5′-ACACCCACCATGCACCAAGT-3′; *PomcCre* primers: N16R: 5′-TGGCTCAATGTCCTTCCTGG-3′; N57R: 5′-CACATAAGC TGCATCGTTAAG-3′; AA03: 5′-GAGATATCTTTAACCCTGA TC-3′; IR-3′: 5′-CTGAATAGCTGAGACCACAG-3′; IR-5′: 5′-GATGTGCACCCCATGTCTG-3′; IR-Δ-5′: 5′-GGGTAGGAA ACAGGATGG-3′. The mice were fed a regular chow diet (Rodent Diet 5001; LabDiet, St. Louis, MO) or an HFD that provides 60% of calories from fat (D12492; Research Diets, New Brunswick, NJ). For the HFD studies, the animals were fed the HFD for 5 months. Animals were housed at an ambient temperature of 21–23°C with a 12-h light-dark cycle (lights on at 0700 h, off at 1900 h). All protocols were approved by the Icahn School of Medicine at Mount Sinai Institutional Animal Care and Use Committee in accordance with guidelines established by the National Institutes of Health.

Hyperinsulinemic-Euglycemic Clamps

At 5 days after implantation of a jugular vein catheter (15), mice were studied through hyperinsulinemic-euglycemic clamps. Food was removed at 9 A.M., and animals were connected to catheters at 11 A.M. when the infusions started. To determine glucose and glycerol fluxes, primed-continuous infusions of [U-^{13}C-6]-D-glucose (0.6 μmol * kg^{-1} * min^{-1}) and [^{2}H-5]-glycerol (4 μmol * kg^{-1} * min^{-1}) were started at t = −100 min, at which time baseline plasma was collected, and the tracer infusions were continued until t = 120 min. Human insulin (Novolin; Novo Nordisk, Princeton, NJ) was primed (72 mU * kg^{-1} * min^{-1}) at t = 0 min for 1 min and then continuously infused at 4 mU * kg^{-1} * min^{-1} for 2 h. Blood glucose was monitored every 10 min, and 25% dextrose was infused at a variable rate to maintain euglycemia. Blood (60 μL) was collected into EDTA tubes at multiple times through tail nicks and processed for measuring plasma insulin and lipids. Animals were anesthetized with isoflurane and sacrificed at the end of the clamps (22). Perigonadal adipose tissues and livers were harvested, snap-frozen in liquid nitrogen, and stored at −80°C until further analysis

Glucose and Glycerol Fluxes

The fluxes were determined as previously described (23). R_a glycerol or glucose (μmol * kg^{-1} * min^{-1}) was calculated by the equation R_a = (MPEinf/MPEpl − 1) × R, where *MPEinf* is the fractional isotopic enrichment of the infused D_5-glycerol or [$^{13}C_6$] glucose in mass percentage excess (MPE), *MPEpl* is the enrichment in the plasma sample (15) and R is the rate of isotope infusion in μmol * kg^{-1} * min^{-1}.

Indirect Calorimetry

To assess energy expenditure and respiratory exchange ratio (RER), the mice were placed in metabolic cages for indirect calorimetry (TSE Systems, Inc., Chesterfield, MO) for 5 days. Animals were fed chow diet and water ad libitum and acclimatized for 3 days. Mice were single-housed in gas-tight cages with a flow rate of 0.40 L/min. The O_2 and CO_2 gas exchange was measured at a 40-s sampling rate per cage. Physical activity was determined concurrently using a one-dimensional infrared light beam system installed on the bottom of the cages.

Glucose Tolerance Test

After a 5-h fast, HFD-fed animals were injected intraperitoneally with 15% glucose solution (0.8 g/kg body wt). Blood glucose was determined in tail vein samples using a hand-held glucometer (OneTouch Ultra; LifeScan, Milpitas, CA) at t = 0, 15, 30, 60, 90, and 120 min.

Cold Tolerance Test

After rectal temperature was measured at ambient room temperature with a small rectal thermometer probe (BAT MO-15; Physitemp, Clifton, NJ), single-housed animals were moved to a cold room at 4°C, and their rectal temperature was measured every 30 min for 2 h.

Hepatic Triglyceride Extraction

Folch triglyceride (TG) extraction was performed as previously described (24–26). Briefly, liver tissues (100 mg) were homogenized in 3 mL of a mixture of methanol and chloroform (1:2 ratio). After incubation for 4 h, 1.5 mL of 0.1 mol/L NaCl was added to the homogenates, and samples were vortexed. After centrifugation at 1,000 rpm for 10 min at room temperature, the lower organic phase

containing TGs was transferred to a new tube, followed by evaporation of the organic solvent with nitrogen gas. Finally, 200 μL of 3 mol/L KOH in 65% ethanol was added to the extracted TGs, and the samples were incubated at 70°C for 1 h.

RNA Extraction and Quantitative Real-time PCR

Total RNA from liver was extracted and processed as previously described (23). Data were analyzed with the comparative C_t method (27). The sequences of quantitative real-time PCR primers were as follows: *IL-6*, 5′-AG TTGCCTTCTTGGGACTGA-3′ (forward) and 5′-ACAGTGCA TCATCGCTGTTC-3′ (reverse); *18S*, 5′-GGGACTTAATCAAC GCAAGC-3′ (forward) and 5′-GTGGAGCGATTTGTCTGGTT (reverse).

Insulin ELISA

Plasma insulin levels were determined with Mercodia Insulin ELISA according to the manufacturer's protocol. Data were analyzed by performing cubic spline regression with Prism (GraphPad Software).

Other Biochemical Measurements

Blood glucose during clamps was measured by hand-held glucometer as indicated above. Plasma free-glycerol and TGs were measured with a colorimetric assay (Triglycerides Kit; Sigma-Aldrich, St. Louis, MO), and plasma nonesterified fatty acid (NEFA) was measured with a colorimetric assay (HR Series NEFA; Wako Chemicals, Richmond, VA).

Statistics

Blood glucose, GIR, R_a glycerol, total VO_2, RER, and body temperature were analyzed by two-way repeated-measures ANOVA, with treatment as a between-subject factor and time as a within-subject factor, followed by Bonferroni post hoc multiple comparisons. hGP was analyzed by two-way ANOVA, followed by Bonferroni post hoc. Plasma insulin, lipids, R_d glucose, percentage suppression of hGP, average VO_2 and RER, locomotor activity, protein expressions in Western blots, and mRNA expression of interleukin 6 (IL-6) were analyzed by Student *t* test to compare the mean difference between AgRP IR KO or POMC IR KO mice and their respective wild-type (WT) littermates. All data are expressed as mean ± SEM. Any statistically significant difference was set at $P < 0.05$.

RESULTS

Insulin Signaling in AgRP Neurons Governs Insulin Action in the Liver but Not in Adipose Tissue

To study the role of insulin signaling in AgRP neurons in regulating systemic insulin action, we crossed mice that were floxed for the IR with mice that expressed Cre recombinase under the control of the AgRP promoter. As a result, the IR gene was excised as confirmed by genomic PCR. These mice are similar to a previously generated AgRP IR KO mouse (9), with the modification that the AgRP Cre used in our study has an internal ribosome entry site that reduces early embryonic deletion of the IR (28).

Body weights of AgRP IR KO mice and littermate controls were similar (g; AgRP IR WT: 33.6 ± 0.9; AgRP IR KO: 35.8 ± 1.7). When we subjected 4-month-old male mice to hyperinsulinemic-euglycemic clamps (Fig. 1*A*), euglycemia was similarly maintained in AgRP IR KOs and their WT littermates (Fig. 1*B*) during the hyperinsulinemic phase, and plasma insulin levels were also similarly raised in both groups (Fig. 1*I*). However, the GIR required to maintain euglycemia in AgRP IR KO mice was significantly lower compared with the WT mice (Fig. 1*C* and *D*), indicative of impaired glucoregulatory insulin action. Indeed, the ability of insulin to suppress hGP was impaired in AgRP IR KO mice, as demonstrated by the lower suppression of hGP during the hyperinsulinemic clamps (Fig. 1*F* and *G*), whereas basal hGP was similar between the groups. The increase in the glucose utilization rate, as assessed by the R_d, was comparable in AgRP IR KO mice and controls during the hyperinsulinemic phase (Fig. 1*E*). These findings demonstrate that insulin action in AgRP neurons governs hepatic insulin action without affecting peripheral glucose utilization, which is congruent with the observation that although insulin infusion into the MBH is able to suppress hGP, it does not increase glucose utilization in rats (15). These results also corroborate a previous clamp study in a different model of AgRP IR KO mice, as mentioned above (9).

Brain insulin action has been suggested to control hGP through the induction of IL-6, which causes phosphorylation and activation of the transcription factor STAT-3 in the liver, which then regulates the expression of gluconeogenic genes (29). To test whether the impaired suppression of hGP in AgRP IR KO mice is caused by reduced hepatic IL-6 expression, we determined IL-6 mRNA levels in the livers of these mice at the end of the clamps. There was no difference in hepatic IL-6 mRNA expression between the groups (Fig. 1*M*), suggesting that the impaired hGP in the AgRP IR KO mice was not caused by impaired hepatic IL-6 expression.

We next assessed the ability of insulin to suppress whole-body lipolysis during the hyperinsulinemic clamps by determining R_a glycerol levels, which provide an estimate of adipose tissue lipolysis. R_a glycerol was not different between the groups during the hyperinsulinemic clamps, indicative of intact adipose tissue insulin action in AgRP IR KO mice. This was also reflected in unaltered plasma TG, glycerol, and NEFAs in the two groups (Fig. 1*H* and *J–L*).

Deletion of IR in POMC Neurons Impairs Insulin Action in Adipose Tissue but Not in the Liver

We next studied the role of insulin signaling in POMC neurons in governing insulin action in the liver and adipose tissue. To delete the IR in POMC neurons, we crossed mice that are floxed for the IR with mice that express Cre recombinase under the control of the POMC promoter (13,30).

Body weights of POMC IR KO mice were similar to those of littermate controls (g; POMC IR WT: 32.0 ± 0.5;

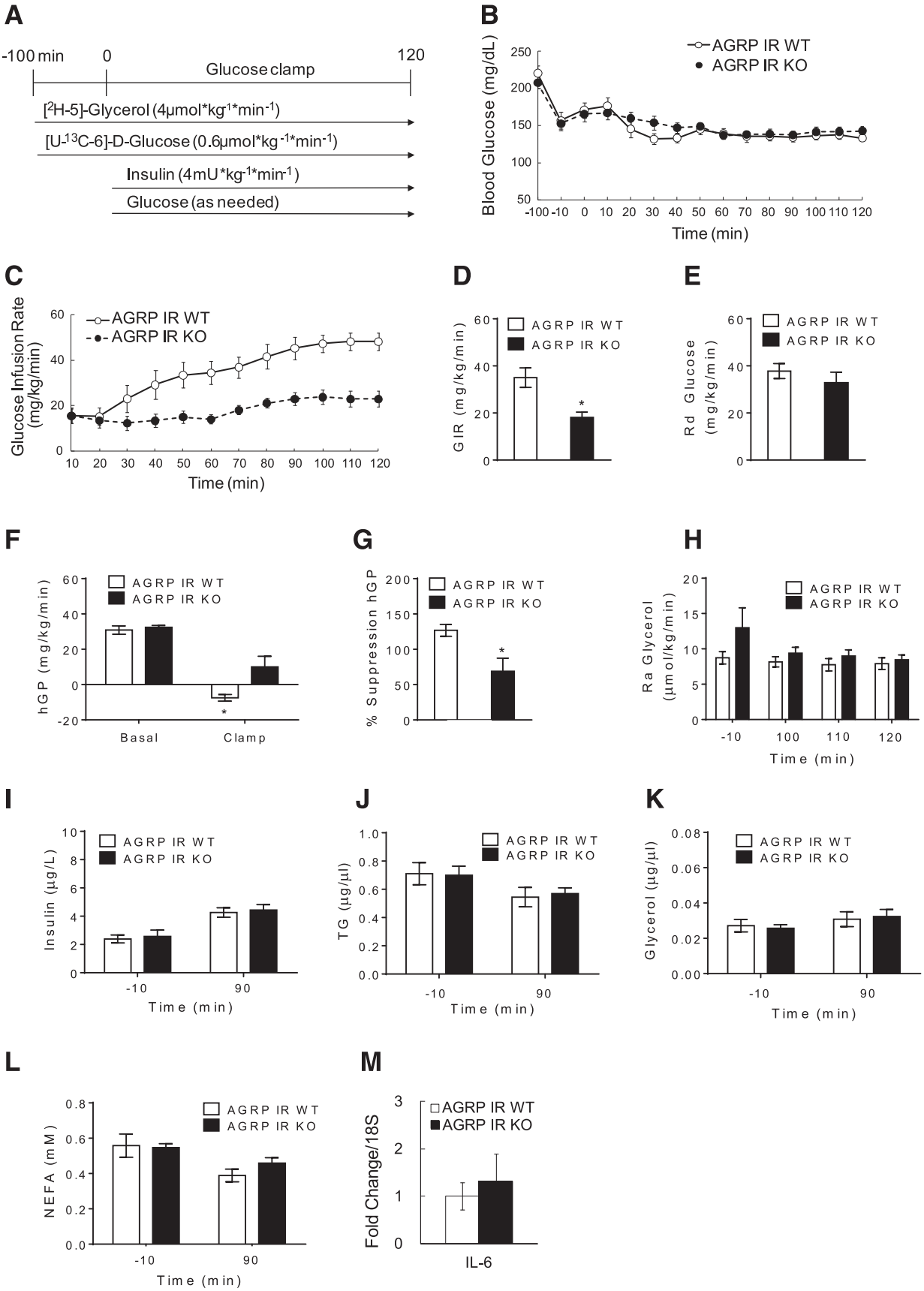

Figure 1—Deletion of IR in AgRP neurons impairs the ability of insulin to suppress HGP without affecting adipose tissue insulin action. *A*: Schematic representation of hyperinsulinemic-euglycemic clamp protocol in mice. *B*: Blood glucose of AgRP IR WT and AgRP IR KO mice before and during the clamp period. *C*: GIR required to maintain euglycemia during the hyperinsulinemic clamps. *D*: Mean GIR. *E*: R_d of

POMC IR KO: 32.7 ± 0.7). Hyperinsulinemic-euglycemic clamps were performed (Fig. 1*A*), during which euglycemia was equally maintained and plasma insulin levels were similarly raised in POMC IR KO and WT littermates (Fig. 2*A* and *H*). Although GIR tended to be lower in POMC IR KO mice, this did not reach statistical significance (Fig. 2*B* and *C*). Hyperinsulinemia similarly increased the glucose utilization rate as assessed by R_d (Fig. 2*D*) and suppressed hGP (Fig. 2*E*) in POMC IR KOs and WT littermates. Hepatic IL-6 mRNA expression was also similar between POMC IR KO mice and the controls (Fig. 2*L*).

Interestingly, R_a glycerol steadily increased in POMC IR KO mice compared with the controls during the clamps, which is likely a result of the moderate stress that all mice experience during the repeated tail vein blood sampling, whereas this increased lipolysis in the WT littermates was prevented through the action of insulin (Fig. 2*G*). This indicates that POMC IR KO mice have impaired adipose tissue insulin action. Despite this difference in lipolysis, plasma lipid levels were not different between POMC IR KO and WT controls (Fig. 2*I–K*).

POMC IR KO but Not AgRP IR KO Mice Display Preferential Fat Utilization

The finding that plasma NEFA levels were not altered in POMC IR KO mice, despite an increased lipolytic rate, suggested that these mice have a higher fatty acid utilization rate that may allow them to maintain normal plasma NEFA levels. To determine the RER, which provides an assessment of the relative carbohydrate versus fatty acid utilization rate, we subjected POMC and AgRP IR KO mice to a metabolic chamber study and measured RER via indirect calorimetry (31). Although total energy expenditure (VO_2) and locomotor activity were not different between POMC IR KO mice, AgRP IR KO mice, and their respective littermate controls (Fig. 3*A, B,* and *E*), the POMC IR KO mice exhibited a significantly lower RER compared with their WT littermates (Fig. 3*C* and *D*), indicative of a higher lipid utilization rate. Hence, POMC IR KO mice are able to maintain normal plasma NEFA levels, despite impaired adipose tissue insulin action, by increasing fatty acid utilization.

Brown adipose tissue is a key organ for thermogenesis and depends primarily on fatty acids as energy substrates. We asked whether increased fat oxidation may confer a higher thermogenic capacity and allow mice to better adapt to a cold environment. To test this, we performed a cold tolerance test in both AgRP and POMC IR KO mice and their WT littermates during which the animals were placed in a cold room (4°C) for 2 h and their rectal temperature was measured every 30 min. Body core temperature was not different in all four groups (Fig. 3*F*), thus demonstrating that the preferential fatty acid utilization failed to augment thermogenesis during cold exposure.

Prolonged HFD Feeding in POMC IR KO Mice Increases Hepatic Steatosis Without Affecting Glucose Tolerance

HFD feeding disrupts glucose and lipid homeostasis by inducing insulin resistance and is a commonly used metabolic stressor to model metabolic syndrome. HFD feeding impairs adipose tissue insulin action, and the resultant increase in lipolytic flux from adipose tissue is an important determinant of hepatic TG content (20). Because POMC IR KO mice exhibit impaired adipose tissue insulin action resulting in unrestrained lipolysis, we hypothesized that they would exhibit an increased susceptibility to HFD-induced hepatic steatosis. To test this, we fed animals a 60% HFD for 5 months. The body weight in both AgRP IR and POMC IR KO mice increased similar to their WT littermates (Fig. 4*A*). There was no difference in fat mass between the KOs and their respective WT littermates (g; AgRP IR WT: 14.0 ± 3.0; AgRP IR KO: 15.4 ± 1.7; POMC IR WT: 14.0 ± 2.5; POMC IR KO: 15.8 ± 5.4). We did not observe any difference in glucose tolerance between both strains and their littermate controls (Fig. 4*B*), as shown by others (9). Plasma NEFA levels were higher in AgRP IR KO mice compared with their WT littermates, although TG or free glycerol levels were comparable (Fig. 4*C*). Importantly, hepatic TG levels in POMC IR KO mice were increased compared with their littermate controls, whereas plasma lipid levels were similar (Fig. 4*E* and *F*). Hepatic protein expression of enzymes involved in lipogenesis, such as fatty acid synthase and acetyl-CoA carboxylase, were not different between POMC IR KO mice and their littermate controls (data not shown), suggesting that the increased hepatic TG levels are not caused by de novo fatty acid synthesis in the liver but are likely the result of an increased influx of fatty acids originating from adipose tissue. Hepatic TG levels in AgRP IR KO mice, however, were similar to those in their WT littermates (Fig. 4*D*). Plasma corticosterone levels were not different between groups (pg/mL; AgRP IR WT: 634 ± 52; AgRP IR KO: 450 ± 109; POMC IR WT: 729 ± 281; POMC IR KO: 690 ± 302), suggesting that the above findings are not attributable to stress responses induced by POMC neurons.

Circulating levels of branched-chain amino acids (BCAAs) are higher in obese individuals (32), and they are the earliest and most predictive marker of diabetes

glucose. *F*: hGP during basal and clamp periods. *G*: Percentage suppression of hGP. *H*: R_a of glycerol in plasma at basal and steady state during the clamp period. Plasma levels of insulin (*I*), TGs (*J*), glycerol (*K*), and NEFA (*L*) during basal and clamp periods. *M*: IL-6 mRNA expressions in liver after hyperinsulinemic clamps. $n \geq 6$ per group. Values are mean ± SEM. $^*P < 0.05$ compared with WT or basal value of respective group.

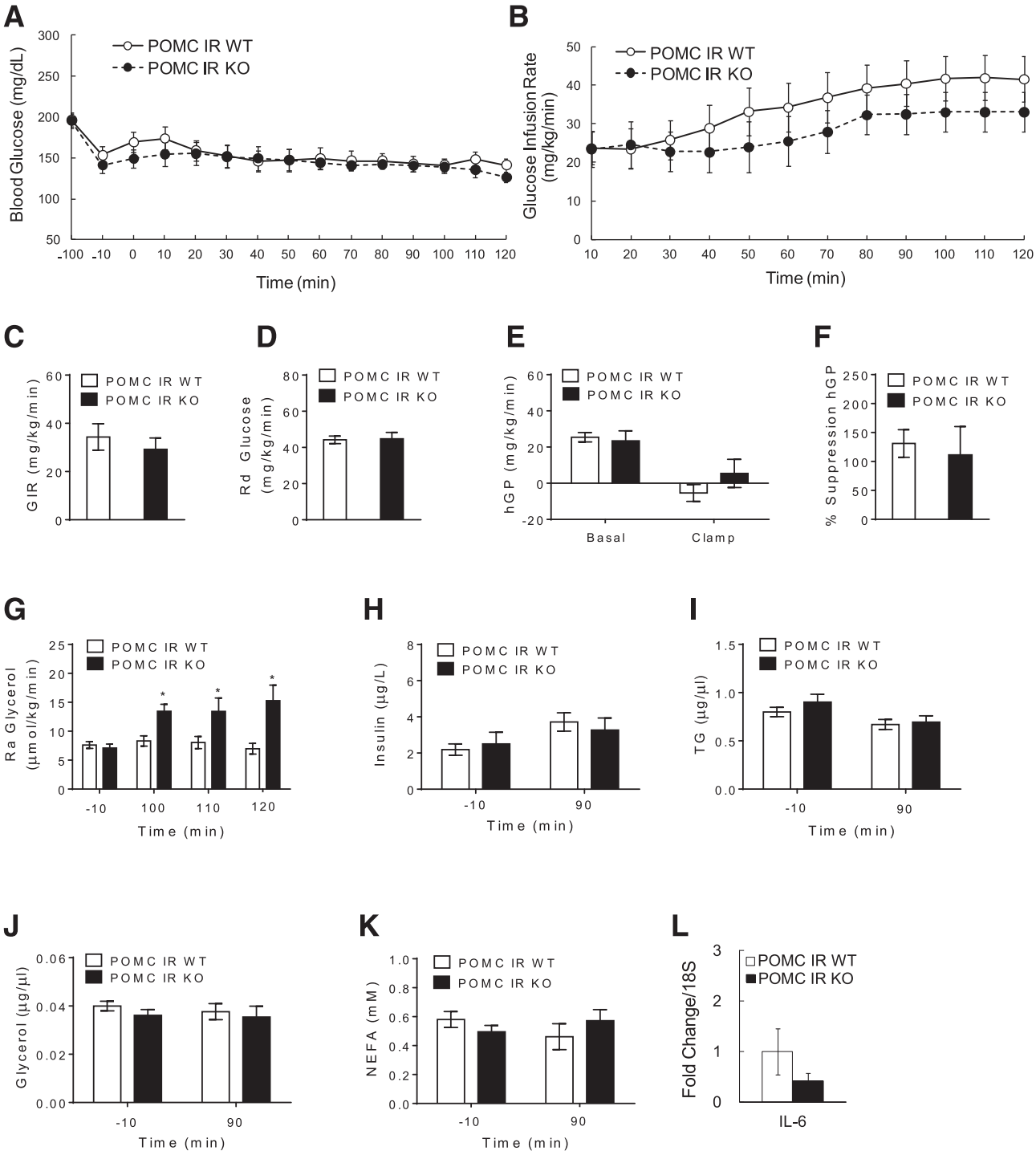

Figure 2—Mice lacking IR in POMC neurons maintain normal hepatic insulin action but display an impaired ability of insulin to suppress lipolysis. *A*: Blood glucose before and during the clamp period. *B*: GIR required to maintain euglycemia during the hyperinsulinemic clamps. *C*: Mean GIR. *D*: R_d of glucose. *E*: hGP during basal and clamp periods. *F*: Percentage suppression of hGP. *G*: R_a of glycerol in plasma at basal and steady state during the clamp period. Plasma levels of insulin (*H*), TGs (*I*), glycerol (*J*), and NEFA (*K*) during basal and clamp periods. *L*: IL-6 mRNA expressions in liver after pancreatic clamps. $n \geq 6$ per group. Values are mean ± SEM. $^*P < 0.05$ compared with WT or basal value of respective group.

(33). We had demonstrated that brain insulin regulates circulating BCAAs by inducing hepatic BCAA catabolism (34). In this study, however, neither AgRP IR nor POMC IR KO mice showed any differences in their plasma BCAA levels before (μmol/L; AgRP IR WT: 633 ± 43; AgRP IR KO: 568 ± 20; POMC IR WT: 978 ± 44; POMC IR KO:

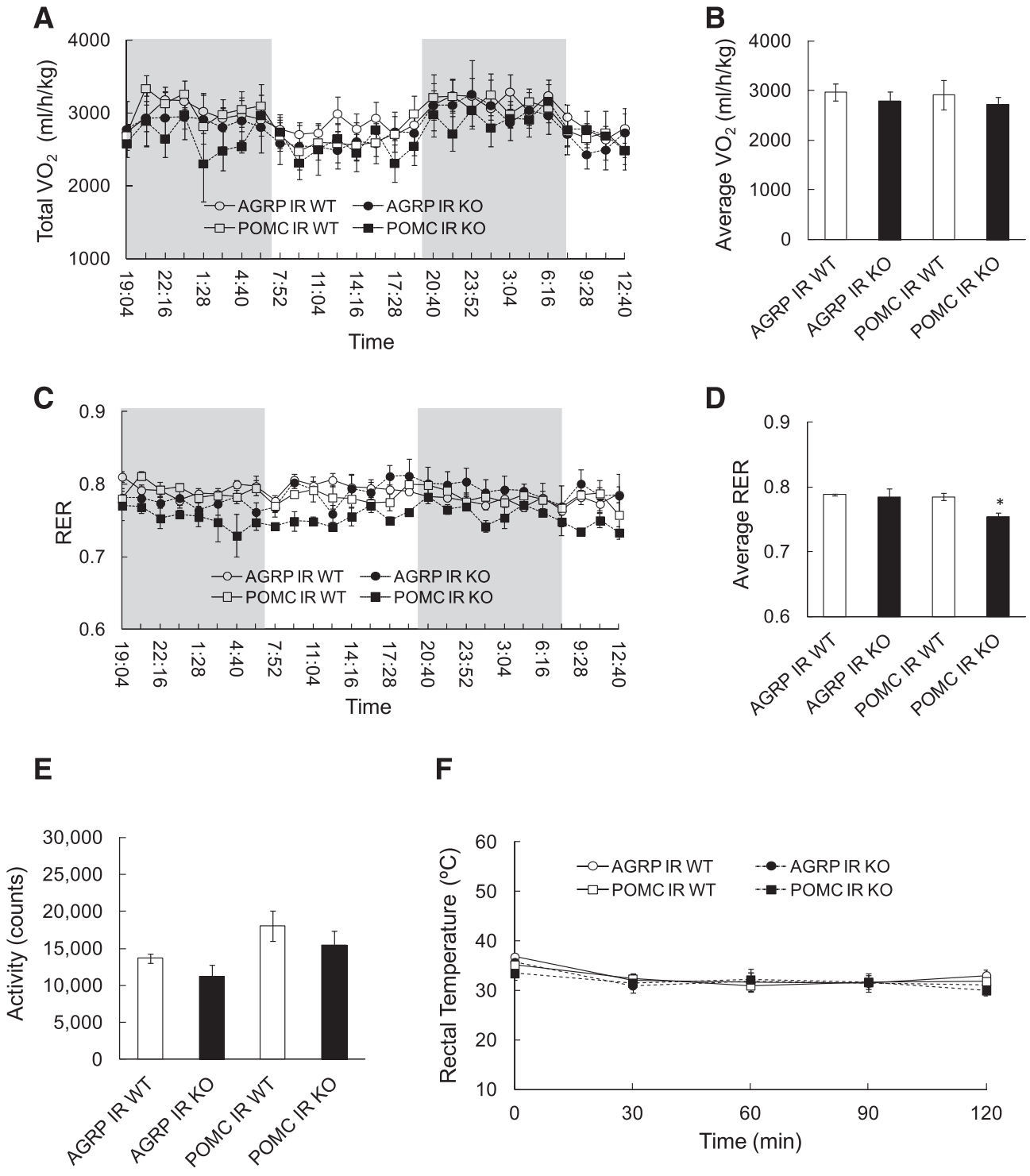

Figure 3—POMC IR KO mice have increased fatty acid utilization rates. *A*: Energy expenditure of AgRP IR KO, POMC IR KO mice, and their respective WT littermates, as measured by total VO_2 consumption in metabolic chambers via indirect calorimetry. *B*: Average VO_2 between groups. *C*: RER measurement. *D*: Average RER. *E*: Locomotor activity in metabolic chambers. *F*: Rectal temperature (°C) of mice during cold tolerance test at 4°C for 2 h. $n \geq 6$ per group. Values are mean ± SEM. $^*P < 0.05$ compared with respective WT.

898 ± 114) or during clamps (AgRP IR WT: 696 ± 36; AgRP IR KO: 700 ± 43; POMC IR WT: 1057 ± 83; POMC IR KO: 975 ± 140) compared with controls, suggesting that AgRP or POMC neurons may not participate in central insulin action for the control of systemic BCAA metabolism.

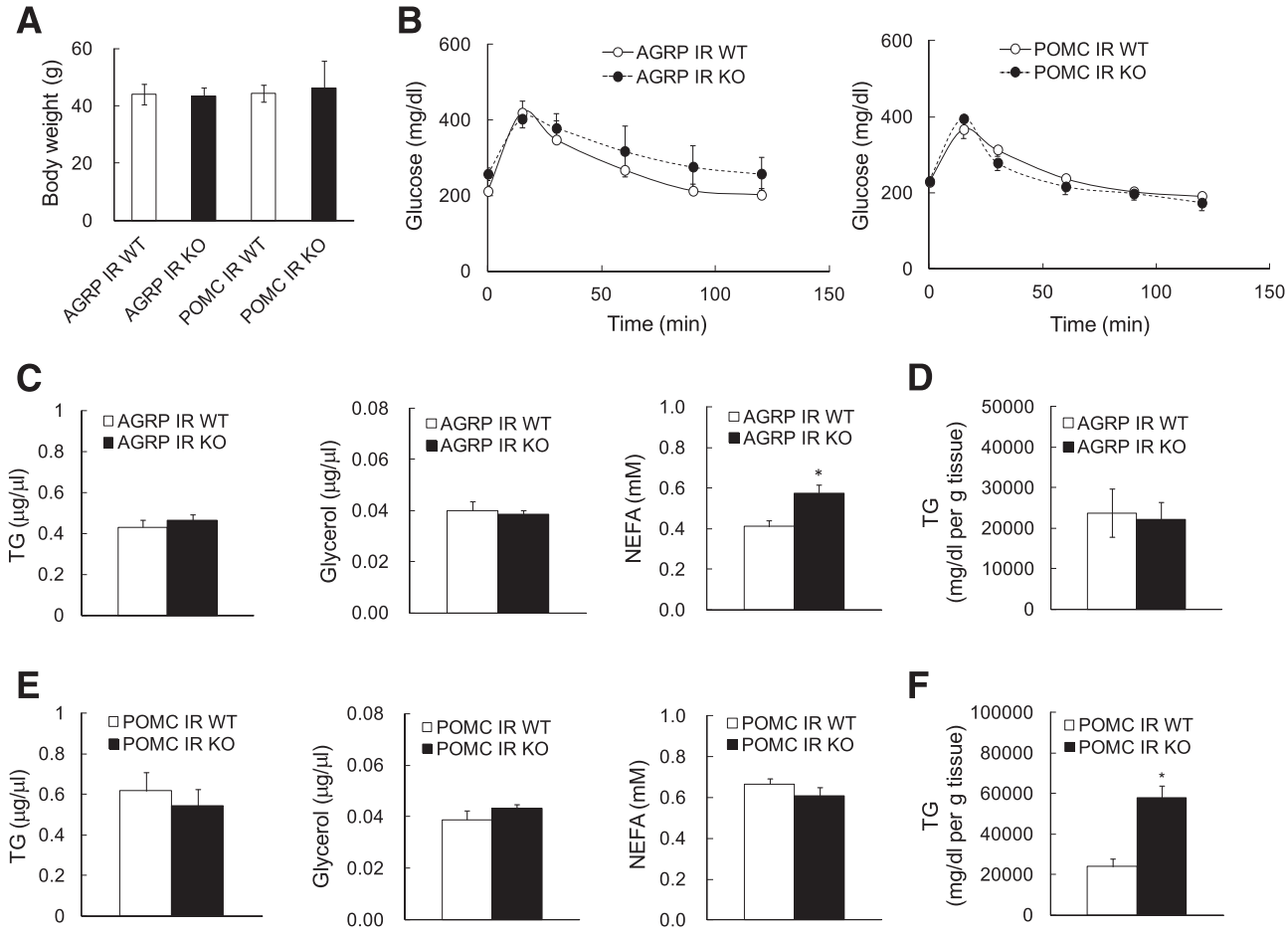

Figure 4—Chronic HFD feeding leads to hepatic steatosis only in POMC IR KO mice without affecting glucose tolerance. *A*: Body weight in mice lacking IR in AgRP or POMC neurons after 5 months of 60% HFD feeding. *B*: Whole-body glucose metabolism of AgRP IR KO mice and POMC IR KO mice as assessed by glucose tolerance test (intraperitoneal injection of 1.5 g/kg body wt). *C*: Plasma levels of TGs, glycerol, and NEFA of AgRP IR KO mice at the time of sacrifice. *D*: TG levels in liver of AgRP IR KO mice. *E*: Plasma levels of TGs, glycerol, and NEFA of POMC IR KO mice at the time of sacrifice. *F*: TG levels in liver of POMC IR KO mice. $n \geq 6$ per group. Values are mean ± SEM. *$P < 0.05$ compared with respective WT.

DISCUSSION

AgRP and POMC neurons are well known for their role in regulating food-seeking behavior, but their role in regulating nutrient partitioning is unclear. In this study, we asked whether insulin signaling in AgRP or POMC neurons regulates systemic glucose and lipid fluxes. We used tracer dilution techniques during hyperinsulinemic clamps to assess glucose fluxes and glycerol fluxes, which are considered the gold standard method to assess hepatic glucose flux and adipose tissue lipolysis. Our findings demonstrate that mice lacking insulin signaling in AgRP neurons exhibit impaired hepatic insulin action, while the ability of insulin to suppress adipose tissue lipolysis remains intact. To the contrary, insulin signaling in POMC neurons does not seem to regulate hepatic insulin action, as indicated by intact insulin-induced suppression of hGP in mice lacking IR in POMC neurons. However, these mice exhibit impaired adipose tissue insulin action, as evidenced by impaired suppression of lipolysis. These findings demonstrate for the first time divergent roles of insulin signaling in AgRP and POMC neurons in regulating glucose versus lipid partitioning. Indeed, susceptibility to HFD-induced fatty liver is increased in POMC IR KO mice where insulin action in adipose tissue is impaired. Hence, impaired insulin action in POMC neurons may provide a novel mechanism by which HFD induces fatty liver, as commonly observed in obese and/or individuals with diabetes, through impaired control of adipose tissue lipolysis (Fig. 5).

Our finding that the ability of insulin to suppress hGP is impaired in AgRP IR KO mice but not in POMC IR KO mice is in agreement with a study by Könner et al. (9), who first found that hepatic insulin action is regulated through insulin signaling in AgRP neurons, although the GIR required to prevent hypoglycemia was unaltered. In our study, the GIR required to prevent hypoglycemia during the hyperinsulinemic clamp was decreased in AgRP IR KO mice,

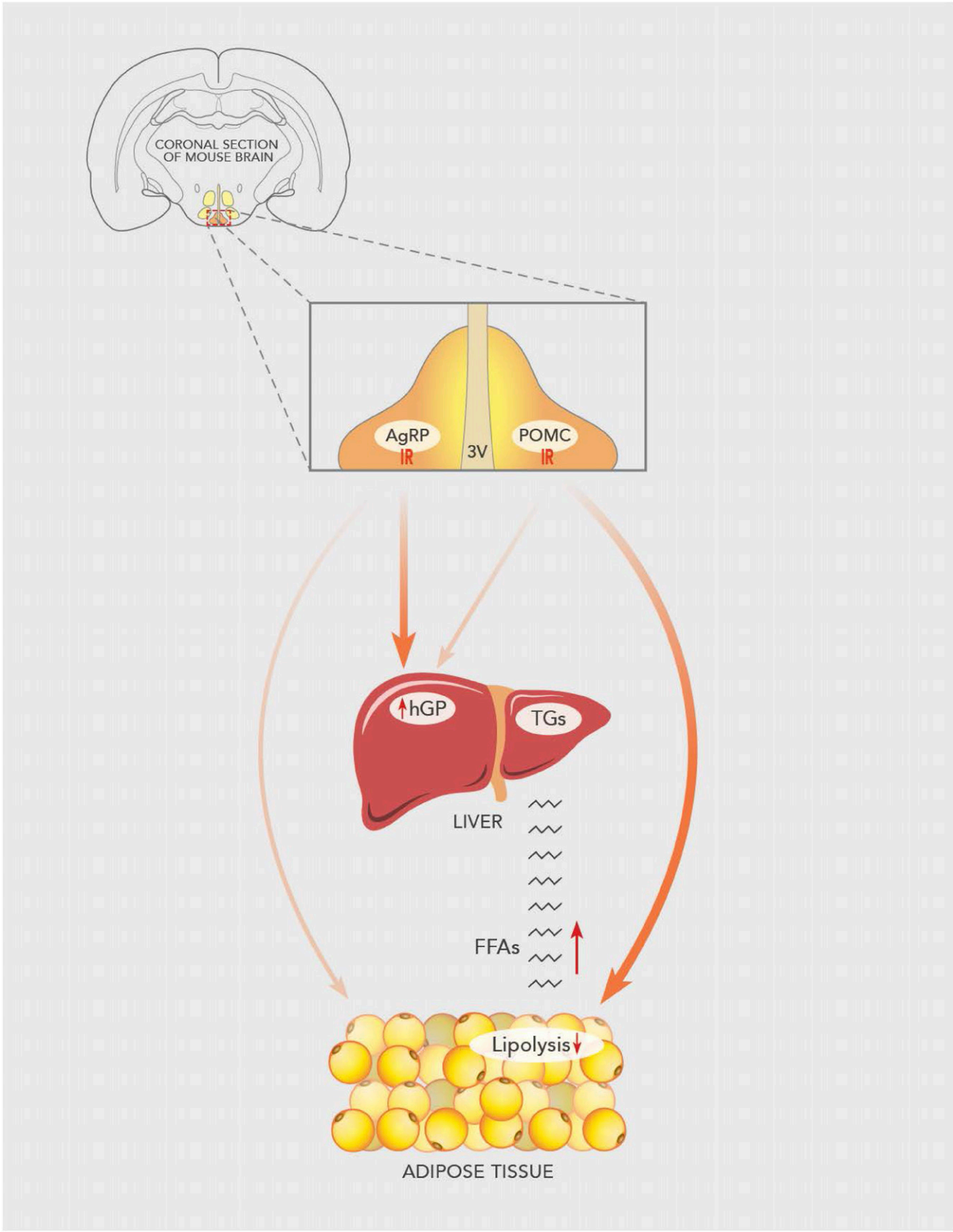

Figure 5—Proposed mechanism. Insulin signaling in AgRP neurons suppresses hGP but does not alter adipose tissue lipolysis. On the other hand, insulin signaling in POMC neurons does not regulate hGP but does restrain adipose tissue lipolysis. Chronic HFD feeding in mice with deletion of IR in POMC neurons exacerbates the lipolysis and increases the flux of free fatty acids (FFAs) into the liver, increasing susceptibility to HFD-induced hepatic steatosis. 3V, 3rd ventricle.

consistent with reduced insulin sensitivity caused by impaired hepatic insulin action. Nevertheless, the difference in GIR between AgRP IR KO mice and the controls is relatively moderate, and in light of the previous finding by Könner et al. that glucose tolerance in the AgRP IR KO mice was maintained, these results suggest that the role of insulin signaling in AgRP neurons is relatively minor compared with the ability of systemic hyperinsulinemia to suppress hGP and to alter glucose homeostasis. Hence, insulin action in other neurons and/or peripheral organs, such as adipose tissue and the liver, may play a dominant role in regulating hepatic glucose fluxes. Hepatic STAT-3 signaling under the control of hepatic IL-6 signaling has been suggested to be a critical component for the ability of central nervous system insulin to suppress hGP (29).

Although Könner et al. (9) have also reported that AgRP IR KO mice exhibit reduced hepatic IL-6 mRNA, we did not find any difference. The reasons for these different results of hepatic IL-6 expression in AgRP IR KO mice may be explained by the significantly longer fasting period before the hyperinsulinemic clamp in the Könner et al. study compared with that in our study (16 h vs. 6 h), because a longer fasting period likely increased gluconeogenic gene expression to a higher level. Hence, the ability of insulin to suppress hGP may also occur independently of hepatic STAT-3/IL-6 signaling.

Insulin has been shown to either stimulate (12) or inhibit (9,10) POMC neurons. Our finding that mice lacking IR in POMC neurons exhibit impaired adipose tissue insulin action resulting in unrestrained lipolysis, along with findings by Brito et al. (21) that melanocortinergic signaling stimulates WAT lipolysis, support the notion that insulin mostly inhibits POMC neurons. It is interesting to note that in our experimental model, adipose tissue lipolysis does not seem to be critical in inducing hepatic insulin resistance, as recently reported by the Shulman group (35), because the ability of insulin to suppress hGP is normal in POMC IR KO mice even though the suppression of lipolysis is impaired.

Another plausible explanation for the lack of hepatic insulin resistance in POMC IR KO mice, despite their unrestrained lipolysis, could be that the circulating glycerol and free fatty acids are readily used by organs other than the liver, thereby maintaining normal plasma levels despite increased lipolysis. Indeed, these mice exhibit unaltered plasma lipid profiles and, importantly, lower RER, which is consistent with preferential lipid oxidation. Hence, POMC IR KO mice seem to have developed a compensatory mechanism to maintain normal circulating lipid levels despite of increased fatty acid mobilization from the adipose tissue, and this may explain the normal hepatic insulin action and glucose tolerance in these mice (9). Hill et al. (13) have shown that neither deletion of the leptin receptor alone nor the combined deletion of the insulin and leptin receptor in POMC neurons alters RER. This would suggest that the IR requires intact leptin receptor signaling in POMC neurons to result in altered RER.

Obese individuals often exhibit increased lipolytic rates compared with lean individuals (36), and the increased lipolytic flux from adipose tissue to the liver can cause hepatic steatosis and systemic insulin resistance (37,38). HFD feeding seems to increase AgRP neuronal activity (39–41) but does not seem to worsen the metabolic phenotype of AgRP IR KO mice, possibly because their AgRP neurons are already disinhibited by the lack of insulin signaling. Although insulin appears to also reduce the firing rate of POMC neurons, HFD feeding increases POMC neuronal activity and/or melanocortinergic tone (42–45), and a lack of insulin signaling in POMC neurons potentiates the dysmetabolic effects of HFD feeding. On the one hand, insulin resistance in POMC neurons during HFD feeding likely results in POMC overactivation, which is an important contributor to the unrestrained lipolysis resulting in hepatic steatosis. On the other hand, we found higher plasma NEFA levels in AgRP IR KO mice during HFD feeding despite no evidence of hepatic steatosis. The elevated NEFA levels may be caused by reduced lipid utilization and/or increased adipose tissue lipolysis.

Impaired lipolytic regulation in POMC IR KO was identified through the use of glycerol tracer dilution technique during insulin clamps. Unrestrained lipolysis is likely the cause of fatty liver that the POMC IR KO mice develop in the setting of HFD feeding. Although assessment of hormone-sensitive lipase and/or perilipin phosphorylation or the level of adiposity is sometimes used to assess lipolysis in adipose tissue, these methods have several limitations, in particular after chronic HFD feeding. First, although hormone-sensitive lipase and perilipin phosphorylation are good markers of lipolysis after an acute lipolytic stimulus, their phosphorylation states are commonly found to be suppressed after HFD feeding (46–49). This may appear at first sight paradoxical because lipolysis is usually increased after HFD feeding, but likely can be attributed to adrenergic desensitization caused by chronic overstimulation. Similarly, fat mass is commonly increased in obesity while lipolysis is unrestrained, and thus, the level of adiposity is not a good indicator of lipolytic regulation. Hence, these disadvantages justify the use of the R_a of glycerol because this method avoids these caveats.

In conclusion, we demonstrate that insulin signaling in POMC neurons plays a critical role in adipose tissue insulin action by restraining lipolysis but seems dispensable for the ability of insulin to suppress hGP. Conversely, insulin signaling in AgRP neurons regulates hGP without affecting adipose tissue lipolysis. Insulin resistance in POMC neurons may play an important role in the development of hepatic steatosis after HFD feeding. Hence, our study demonstrates that insulin signaling in POMC neurons plays a critical role in the regulation of adipose tissue function and in turn in the susceptibility to fatty liver development.

Acknowledgments. The authors thank Wilson Hsieh, from Icahn School of Medicine at Mount Sinai, for technical assistance.

Funding. This study was funded by the National Institute of Diabetes and Digestive and Kidney Diseases grants K01-DK-099463 (A.C.S.) and R01-DK-082724, the National Institute on Alcohol Abuse and Alcoholism grant R01-AA-023416, and the American Diabetes Association grant 7-11-CD-02 (C.B.).

Duality of Interest. No potential conflicts of interest relevant to this article were reported.

Author Contributions. A.C.S. collected and analyzed data, contributed to discussion, and wrote the manuscript. N.F., T.C., S.D., and D.O. collected data. C.L. collected and analyzed data. C.B. conceived the study, supervised the experimentation and data analysis, and wrote the manuscript. C.B. is the guarantor of this work and, as such, had full access to all the data in the study and takes responsibility for the integrity of the data and the accuracy of the data analysis.

References

1. Krashes MJ, Shah BP, Koda S, Lowell BB. Rapid versus delayed stimulation of feeding by the endogenously released AgRP neuron mediators GABA, NPY, and AgRP. Cell Metab 2013;18:588–595

2. Aponte Y, Atasoy D, Sternson SM. AGRP neurons are sufficient to orchestrate feeding behavior rapidly and without training. Nat Neurosci 2011;14:351–355

3. Krashes MJ, Koda S, Ye C, et al. Rapid, reversible activation of AgRP neurons drives feeding behavior in mice. J Clin Invest 2011;121:1424–1428

4. Bewick GA, Gardiner JV, Dhillo WS, et al. Post-embryonic ablation of AgRP neurons in mice leads to a lean, hypophagic phenotype. FASEB J 2005;19:1680–1682

5. Gropp E, Shanabrough M, Borok E, et al. Agouti-related peptide-expressing neurons are mandatory for feeding. Nat Neurosci 2005;8:1289–1291

6. Luquet S, Perez FA, Hnasko TS, Palmiter RD. NPY/AgRP neurons are essential for feeding in adult mice but can be ablated in neonates. Science 2005;310:683–685

7. Zhan C, Zhou J, Feng Q, et al. Acute and long-term suppression of feeding behavior by POMC neurons in the brainstem and hypothalamus, respectively. J Neurosci 2013;33:3624–3632

8. Koch M, Varela L, Kim JG, et al. Hypothalamic POMC neurons promote cannabinoid-induced feeding. Nature 2015;519:45–50

9. Könner AC, Janoschek R, Plum L, et al. Insulin action in AgRP-expressing neurons is required for suppression of hepatic glucose production. Cell Metab 2007;5:438–449

10. Williams KW, Margatho LO, Lee CE, et al. Segregation of acute leptin and insulin effects in distinct populations of arcuate proopiomelanocortin neurons. J Neurosci 2010;30:2472–2479

11. Claret M, Smith MA, Batterham RL, et al. AMPK is essential for energy homeostasis regulation and glucose sensing by POMC and AgRP neurons. J Clin Invest 2007;117:2325–2336

12. Qiu J, Zhang C, Borgquist A, et al. Insulin excites anorexigenic proopiomelanocortin neurons via activation of canonical transient receptor potential channels. Cell Metab 2014;19:682–693

13. Hill JW, Elias CF, Fukuda M, et al. Direct insulin and leptin action on proopiomelanocortin neurons is required for normal glucose homeostasis and fertility. Cell Metab 2010;11:286–297

14. Koch L, Wunderlich FT, Seibler J, et al. Central insulin action regulates peripheral glucose and fat metabolism in mice. J Clin Invest 2008;118:2132–2147

15. Scherer T, O'Hare J, Diggs-Andrews K, et al. Brain insulin controls adipose tissue lipolysis and lipogenesis. Cell Metab 2011;13:183–194

16. Scherer PE. The multifaceted roles of adipose tissue-therapeutic targets for diabetes and beyond: the 2015 Banting Lecture. Diabetes 2016;65:1452–1461

17. Ono H, Pocai A, Wang Y, et al. Activation of hypothalamic S6 kinase mediates diet-induced hepatic insulin resistance in rats. J Clin Invest 2008;118:2959–2968

18. Pocai A, Morgan K, Buettner C, Gutierrez-Juarez R, Obici S, Rossetti L. Central leptin acutely reverses diet-induced hepatic insulin resistance. Diabetes 2005;54:3182–3189

19. Wang J, Obici S, Morgan K, Barzilai N, Feng Z, Rossetti L. Overfeeding rapidly induces leptin and insulin resistance. Diabetes 2001;50:2786–2791

20. Scherer T, Lindtner C, Zielinski E, O'Hare J, Filatova N, Buettner C. Short term voluntary overfeeding disrupts brain insulin control of adipose tissue lipolysis. J Biol Chem 2012;287:33061–33069

21. Brito MN, Brito NA, Baro DJ, Song CK, Bartness TJ. Differential activation of the sympathetic innervation of adipose tissues by melanocortin receptor stimulation. Endocrinology 2007;148:5339–5347

22. Okamoto H, Obici S, Accili D, Rossetti L. Restoration of liver insulin signaling in Insr knockout mice fails to normalize hepatic insulin action. J Clin Invest 2005;115:1314–1322

23. Lindtner C, Scherer T, Zielinski E, et al. Binge drinking induces whole-body insulin resistance by impairing hypothalamic insulin action. Sci Transl Med 2013;5:170ra14

24. Folch J, Lees M, Sloane Stanley GH. A simple method for the isolation and purification of total lipides from animal tissues. J Biol Chem 1957;226:497–509

25. Kraus D, Yang Q, Kahn BB. Lipid extraction from mouse feces. Bio Protoc 2015;5:e1375

26. Mokler FT, Lin Q, Luo H, et al. Dual-label studies with [^{125}I]-3(R)/[^{131}I]-3(S)-BMIPP show similar metabolism in rat tissues. J Nucl Med 1999;40:1918–1927.

27. Schmittgen TD, Livak KJ. Analyzing real-time PCR data by the comparative C(T) method. Nat Protoc 2008;3:1101–1108

28. Tong Q, Ye CP, Jones JE, Elmquist JK, Lowell BB. Synaptic release of GABA by AgRP neurons is required for normal regulation of energy balance. Nat Neurosci 2008;11:998–1000

29. Inoue H, Ogawa W, Asakawa A, et al. Role of hepatic STAT3 in brain-insulin action on hepatic glucose production. Cell Metab 2006;3:267–275

30. Balthasar N, Coppari R, McMinn J, et al. Leptin receptor signaling in POMC neurons is required for normal body weight homeostasis. Neuron 2004;42:983–991

31. Lin HV, Plum L, Ono H, et al. Divergent regulation of energy expenditure and hepatic glucose production by insulin receptor in agouti-related protein and POMC neurons. Diabetes 2010;59:337–346

32. Newgard CB, An J, Bain JR, et al. A branched-chain amino acid-related metabolic signature that differentiates obese and lean humans and contributes to insulin resistance. Cell Metab 2009;9:311–326

33. Wang TJ, Larson MG, Vasan RS, et al. Metabolite profiles and the risk of developing diabetes. Nat Med 2011;17:448–453

34. Shin AC, Fasshauer M, Filatova N, et al. Brain insulin lowers circulating BCAA levels by inducing hepatic BCAA catabolism. Cell Metab 2014;20:898–909

35. Perry RJ, Camporez JP, Kursawe R, et al. Hepatic acetyl CoA links adipose tissue inflammation to hepatic insulin resistance and type 2 diabetes. Cell 2015;160:745–758

36. Horowitz JF, Klein S. Whole body and abdominal lipolytic sensitivity to epinephrine is suppressed in upper body obese women. Am J Physiol Endocrinol Metab 2000;278:E1144–E1152

37. Samuel VT, Petersen KF, Shulman GI. Lipid-induced insulin resistance: unravelling the mechanism. Lancet 2010;375:2267–2277

38. Yki-Järvinen H. Ectopic fat accumulation: an important cause of insulin resistance in humans. J R Soc Med 2002;95(Suppl. 42):39–45

39. Baver SB, Hope K, Guyot S, Bjørbaek C, Kaczorowski C, O'Connell KM. Leptin modulates the intrinsic excitability of AgRP/NPY neurons in the arcuate nucleus of the hypothalamus. J Neurosci 2014;34:5486–5496

40. Dietrich MO, Liu ZW, Horvath TL. Mitochondrial dynamics controlled by mitofusins regulate Agrp neuronal activity and diet-induced obesity. Cell 2013;155:188–199

41. Wei W, Pham K, Gammons JW, et al. Diet composition, not calorie intake, rapidly alters intrinsic excitability of hypothalamic AgRP/NPY neurons in mice. Sci Rep 2015;5:16810
42. Bergen HT, Mizuno T, Taylor J, Mobbs CV. Resistance to diet-induced obesity is associated with increased proopiomelanocortin mRNA and decreased neuropeptide Y mRNA in the hypothalamus. Brain Res 1999;851:198–203
43. Enriori PJ, Evans AE, Sinnayah P, et al. Diet-induced obesity causes severe but reversible leptin resistance in arcuate melanocortin neurons. Cell Metab 2007;5:181–194
44. Huang XF, Han M, South T, Storlien L. Altered levels of POMC, AgRP and MC4-R mRNA expression in the hypothalamus and other parts of the limbic system of mice prone or resistant to chronic high-energy diet-induced obesity. Brain Res 2003;992:9–19
45. Lee AK, Mojtahed-Jaberi M, Kyriakou T, et al. Effect of high-fat feeding on expression of genes controlling availability of dopamine in mouse hypothalamus. Nutrition 2010;26:411–422
46. Ray H, Pinteur C, Frering V, Beylot M, Large V. Depot-specific differences in perilipin and hormone-sensitive lipase expression in lean and obese. Lipids Health Dis 2009;8:58
47. Rydén M, Jocken J, van Harmelen V, et al. Comparative studies of the role of hormone-sensitive lipase and adipose triglyceride lipase in human fat cell lipolysis. Am J Physiol Endocrinol Metab 2007;292:E1847–E1855
48. Steinberg GR, Kemp BE, Watt MJ. Adipocyte triglyceride lipase expression in human obesity. Am J Physiol Endocrinol Metab 2007;293:E958–E964
49. Moreno-Navarrete JM, Ortega F, Serrano M, et al. CIDEC/FSP27 and PLIN1 gene expression run in parallel to mitochondrial genes in human adipose tissue, both increasing after weight loss. Int J Obes 2014;38:865–872